Energy-aware Terrain Analysis for Mobile Robot Exploration

Kyohei Otsu and Takashi Kubota

Abstract This paper presents an approach to predict energy consumption in mobility systems for wheeled ground robots. The energy autonomy is a critical problem for various battery-powered systems. Specifically, the consumption prediction in mobility systems, which is difficult to obtain due to its complex interactivity, can be used to improve energy efficiency. To address this problem, a self-supervised approach is presented which considers terrain geometry and soil types. Especially, this paper analyzes soil types which affect energy usage models, then proposes a prediction scheme based on terrain type recognition and simple consumption modeling. The developed vibration-based terrain classifier is validated with a field test in diverse volcanic terrain.

1 Introduction

As robotics technology develops rapidly, a number of applications are deployed into real fields. These real-world robotic applications are typically subject to the interaction with a challenging environment, which is characterized by its dynamic and unknown properties. The robots deployed in these fields should have the capability to percept, model, and interact with surrounding situations, in order to enable safe and efficient operations under several hardware restrictions. Such autonomy is to some extent required for any independent systems, especially for robots in extreme environments including planetary surfaces and active volcanoes. Significant examples for extreme terrain operations include the Mars rovers developed by

Kyohei Otsu
Department of Electrical Engineering and Information Systems, The University of Tokyo, 7-3-1 Hongo, Bunkyo, Tokyo, Japan e-mail: kyon@ac.jaxa.jp

Takashi Kubota
Institute of Space and Astronautical Science, Japan Aerospace Exploration Agency, 3-1-1 Yoshinodai, Chuo, Sagamihara, Kanagawa, Japan e-mail: kubota@isas.jaxa.jp

NASA/JPL. The autonomous navigation system have shown successful results on the remote planetary surface without intensive human intervention [2, 11].

Besides the interaction with surroundings, the energy autonomy is an essential technique for battery-powered embedded systems. To enable long-term operations, the robots should be capable to obtain power either from mounted generators or external energy hotspots, and use it properly to perform all assigned tasks. Since the energy budget is severely limited, system designers will face difficult challenges for efficient energy utilization. A battery-powered system is known to survive longer by appropriate scheduling of energy-consuming tasks. For example, an decreasing load profile improves the battery behavior and makes the lifetime longer than an inverse profile [14]. This battery characteristic leads to the following idea: if the energy consumption can be predicted prior to the execution, and the task scheduling is appropriately performed, the exploration period and range might be extended.

The aim of this research is a priori estimation of energy consumption in mobility systems. The energy consumption is associated in some way with the robot mechanical properties and terrain characteristics. One of the challenging problems is to estimate the interaction between a robot and terrain since the soil behavior cannot be modeled uniformly. In the proposed method, a self-supervised scheme is adopted to make a simple model for energy prediction. Firstly, a vibration-based classifier provides the estimation of terrain class which characterize the interaction model. Then, given the class as teacher data, a vision-based classifier gives a priori estimation of the class through machine learning techniques. Finally, the energy consumption is predicted using the terrain class and geometry data.

This paper presents the concept of the proposed scheme and detailed description of energy-aware terrain classification based on vibration signals. The algorithm is tested by real-world data obtained with a four-wheeled vehicle in diverse volcanic terrain.

2 Related Works

The core part of this research belongs to the terrain classification problem. Specifically, vibration-based terrain classification has been conducted by several research groups after it is initially suggested by Iagnemma and Dubowsky [9]. Sadhukhan et al. and DuPont et al. developed a neural network approach using FFT-based vibration analysis, which distinguishes different terrain types [15, 16, 8]. Brooks et al. proposed a classification framework using contact microphones, which estimates terrain components such as sand and gravel [3, 4]. Weiss et al. proposed a feature-based compact representation, which is fairly relevant to this research, classifying different terrain types [20]. Ojeda et al. developed a neural network method applicable to other sensors [12]. Similarly, road roughness estimation was performed for high-speed vehicles by Stavens et al.[17]. These works extract descriptive vectors from raw vibration signals, and utilize machine learning to compute terrain labels. Many of the works are conducted in the frequency domain. Comparisons of different classification methods are given by Weiss et al. [19] and Coyle et al. [7], where they mention high accuracy of the SVM (Support Vector Machine) classifier when paired with proper kernel functions.

Recently, the self-supervised scheme is actively studied and applied to robotics applications. The self-supervised classification is an automatic training of a classifier using estimated labels from other classifiers. The classifier to be trained is usually using remote sensors such as cameras and LIDARs. Angelova et al. performed vision-based unsupervised clustering to obtain terrain labels, then the labels are used to train their slip estimator [1]. Krebs et al. enabled an on-line learning of mobility attributes by combining vision and inertial/mechanical measurements using a Bayesian framework [10]. Brooks et al. proposed a framework to predict mechanical properties of distant terrain by empirical learning of wheel-terrain interaction [5]. Those works successfully predicted terrain attributes of distant terrain.

The research presented in this article also employs self-supervised learning in order to predict energy consumption before the robot actually drives over the terrain. The attribute to be estimated is apparently important for energy-aware behavior planning. However, it is difficult to make accurate estimation since required power is determined by a complex function of the robot and terrain interaction. This paper analyzes the relation of energy consumption and robot-terrain interaction and develops a simple inference model using a vibration sensor and cameras. Based on the model, the energy consumption is predicted for typical wheeled vehicles.

3 Technical Approaches

This section describes the conceptual overview of the system. Then, the detailed technical description is given for the energy-aware terrain analysis using vibration measurements.

3.1 Self-supervised Scheme for Inferencing Energy Consumption

The energy consumption in mobility systems depends on both terrain types and geometry. Let E be the energy consumption, A, G be the appearance and geometry information obtained from cameras, and V be the vibration measurement from an IMU. Assuming the consumption model is specific for finite terrain types, the regression function of energy from inputs can be expressed as

$$f(E|A,G,V) = \sum_T P(T|A,G,V) f(E|T,A,G,V) \tag{1}$$

$$= \sum_T P(T|A,V) f(E|T,G) \tag{2}$$

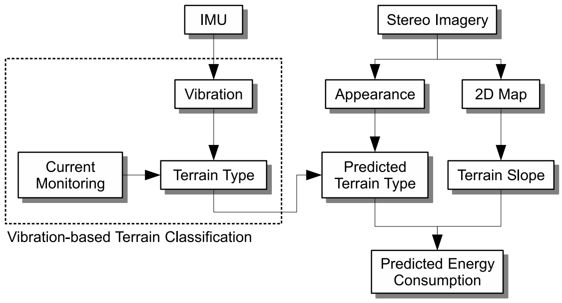

Fig. 1 Overview of self-supervised scheme.

for terrain type T and $\sum_T P(T|A,V) = 1$. From this equation, the problem can be split into the terrain type recognition problem ($P(T|A,V)$) and the energy consumption inference problem ($f(E|T,G)$). For recognizing terrain types, a robot classifies terrain using appearance and vibration measurements. The self-supervised scheme is used in this part, i.e., the terrain labels from the vibration-based classifier are used as teacher data for the vision-based predictive classifier. On the other hand, the regression function is determined empirically from experimental data. The function is developed based on the physical model of typical wheeled robots.

The illustration of the proposed self-supervised scheme is given in Fig. 1. The remainder of this paper focuses on the method to estimate energy consumption based on vibration analysis. Firstly, the function $f(E|T,G)$ is formulated from a physical model. It shows the energy consumption is a linear function that depends on the robot-terrain interaction. Next, the self-supervised classification based on vibration analysis is explained. The classified result is processed in a winner-take-all manner, and combined with the formulated energy equation to provide accurate energy prediction.

3.2 Energy Consumption Model for Wheeled Vehicles

The amount of energy consumption depends on the soil type and the terrain geometry. In this section, the model is explained based on a physical model of wheeled vehicles.

Consider a robot driving in a velocity v over a slanted pseudo plane with angle θ_p (Fig. 2). The vehicle dynamics is expressed by

$$\sum_j f_{dj} - \sum_j f_{rj} - Mg \sin \theta_p = M\dot{v} \tag{3}$$

where F_{dj} is the driving force of each wheel, f_{rj} is the driving resistance of each wheel, M is the total mass of the robot, and g is the gravity constant. The driving resistance f_{rj} is expressed as the sum of rolling resistance between the wheel and terrain $f_{wj}(v)$ and friction loss in bearing and gear $f_{gj}(v)$.

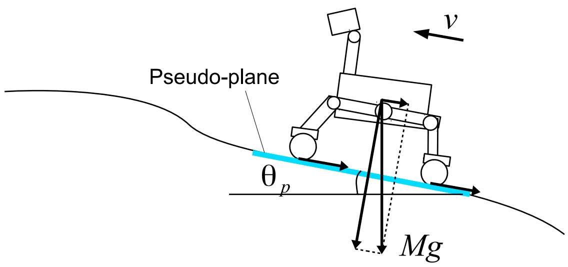

Fig. 2 Wheeled robot model on slanted pseudo plane.

$$F_{rj}(v) = f_{wj}(v) + f_{gj}(v) \tag{4}$$

The resistance depends on the robot velocity. To simplify the problem, let us put an affordable assumption that the robot drives at an arbitrary constant speed v_0 within a small distance. Then, the equation (3) becomes

$$F_d = \sum_j [f_{wj}(v_0) + f_{gj}(v_0)] + Mg\sin\theta_p \tag{5}$$

where F_d is the sum of all driving forces.

On the other hand, the driving force can be computed from the motor torque

$$f_{dj} = \frac{\eta\gamma T_j}{R} \tag{6}$$

where η is the transmission efficiency, γ is the gear reduction ratio, T_j is the generated torque, and R is the wheel radius. Since the torque is proportional to current

$$T_j = k_t I_j \tag{7}$$

the electrical energy consumption is expressed by

$$E_e = \frac{VR\left(\sum_j [f_{wj}(v_0) + f_{gj}(v_0)] + Mg\sin\theta_p\right)}{\eta\ \gamma\ k_t} \tag{8}$$

where V represents the source voltage. Under the assumption that the traversable slope for wheeled robots is small, the equation can be simplified to

$$E_e \simeq \alpha_{r,t} + \beta_r\theta_p \tag{9}$$

where $\alpha_{r,t}$ and β_r is constant values. Note that $\alpha_{r,t}$ depends on both robots and terrain, while β_r depends on only robot systems. However, in the real natural environments, the slope angle observation θ is not consistent with the pseudo plane angle θ_p due to the terrain deformation. In this paper, the deformation effect is modeled by a linear equation as $\theta_p = \gamma_{r,t}\theta$. Hence, the final inference model is expressed as

$$E_e \simeq \alpha_{r,t} + \beta_r \gamma_{r,t} \theta \tag{10}$$
$$= \alpha_{r,t} + \delta_{r,t} \theta \tag{11}$$

The above model suggests that we can infer the energy consumption using two constants and a slope angle measurement. The constants are estimated empirically from experiments. In the preliminary study, they depends on soil types, which can be classified by vibration-based machine learning. On the other hand, the slope angle is computed geometrically from stereo vision. There are several efficient methods to recover terrain geometry from images [13].

3.3 Vibration-based Terrain Classification

In order to know the terrain class and the associated constants which affect energy consumption, a vibration-based terrain classifier is proposed. The reason to choose vibration is that it well represents the wheel-terrain interaction as presented in the previous studies [3, 20], whereas the direct measurement of motor currents does not work due to its high dependency on the terrain geometry (which can also be seen in (11)).

The proposed classifier employes the feature-based SVM similar to [20]. However, the feature representation described here is computed in the frequency domain, and designed to work for a real outdoor robot.

At first, vibration data is collected from an accelerometer rigidly attached to the robot body. Using 3-axis acceleration data the signal power is computed and then subtracted by the short-time averages. The processed time-series acceleration vector $\boldsymbol{a} = [a_1, \cdots, a_t, \cdots]$ is converted to the time-frequency domain by continuous wavelet transform [18].

$$\boldsymbol{A} = \begin{bmatrix} A_{f_1,1} & \cdots & A_{f_1,t} & \cdots \\ \vdots & \ddots & \vdots & \\ A_{f_m,1} & \cdots & A_{f_m,t} & \cdots \end{bmatrix} \tag{12}$$

In this representation, each column corresponds to the signal spectrum for each time, and each row corresponds to the time-series of a single frequency.

The raw matrix can be used to train the classifiers. However, in this paper, the raw matrix is subsampled to $2 \times N$ matrix for sake of efficiency. The rows and columns are selected so that the characteristic elements are preserved. For the frequency domain, the natural frequency f_n and its octave $2f_n$ are preserved. The signal power for the natural frequency is dominant in vibration analysis of the robot locomotion. For the time domain, samples on the grouser-to-grouser interval t_g are selected. Typically, all-terrain robots have grousers to obtain traction. The symmetric arrangement of grousers causes periodical characteristics to signal spectra as shown in Fig. 3. The local peak positions are utilized to describe the time-domain characteristics. N samples around designated time t are extracted.

After the subsample process, the following $2 \times N$ matrix is obtained.

$$\begin{bmatrix} \boldsymbol{x}_{t,f_n} \\ \boldsymbol{x}_{t,2f_n} \end{bmatrix} = \begin{bmatrix} A_{f_n,1} & \cdots & A_{f_n,N} \\ A_{2f_n,1} & \cdots & A_{2f_n,N} \end{bmatrix} \tag{13}$$

For each row vector $\boldsymbol{x}_t$, the following features are extracted.

- The mean μ_t of the vector. The mean is roughly 0 for smooth surfaces, while it becomes grater for rough surfaces.

$$\mu_t = \frac{1}{N}\sum_{i=1}^{N} x_i \tag{14}$$

- The standard deviation σ_t. The larger deviation represents the terrain is not uniformly composed.

$$\sigma_t = \sqrt{\frac{1}{N}\sum_{i=1}^{N}(x_i - \mu_t)^2} \tag{15}$$

- The maximum value m_t of the vector. It corresponds to the strength of the shock from the terrain.

$$m_t = \max(\boldsymbol{x}_t) \tag{16}$$

- The coefficient of variation c_t. It is the relative variance to the signal strength.

$$c_t = \frac{\sigma_t}{\mu_t} \tag{17}$$

Using these four types of features, the feature vector for each time is acquired as follows.

$$\boldsymbol{X}_t = \left[\mu_{t,f_n}\ \sigma_{t,f_n}\ m_{t,f_n}\ c_{t,f_n}\ \mu_{t,2f_n}\ \sigma_{t,2f_n}\ m_{t,2f_n}\ c_{t,2f_n}\right]^\top \tag{18}$$

The 8-element feature vectors are used to train classifiers. Each classifier detects one pre-defined terrain type against all others. Although unsupervised clustering can be used here as in [1], the supervised learning still provides accurate enough estimation of the energy-related constants. Therefore, the supervised SVM is employed for implementation in order to classify different soil sizes.

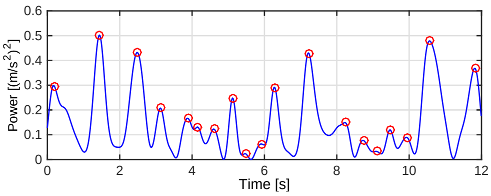

Fig. 3 Time-series signal power corresponding to the natural frequency. Detected positive peaks caused by grouser-to-grouser intervals are marked with red circles.

4 Experiment

In the previous section, the energy inference method based on vibration measurements is presented. The field experiment described in this section shows the validity of the approach and evaluates the performance.

4.1 Setup

The rover used in the field experiment is shown in Fig. 4. It is a four-wheeled unmanned vehicle with a customized suspension system. The dimensions are $0.88 \times 0.83 \times 1.50$ [m] and it weighs 50 [kg]. Four aluminum wheels with silicon grousers are driven by DC motors at a rate 7.6 [rpm]. The wheel radius is 0.10 [m] and the grouser-to-grouser distance is 0.05 [m]. Attached to the body, a 3-axis accelerom-

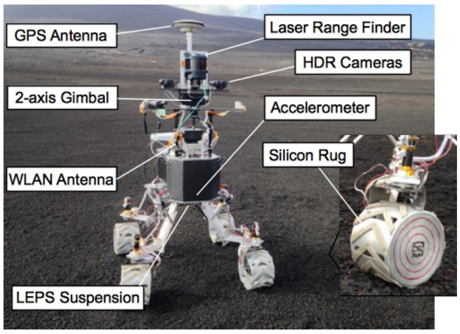

Fig. 4 The AKI rover. Four wheeled all-terrain robots with custom suspension mechanism. Silicon rugs are attached to the aluminum wheels.

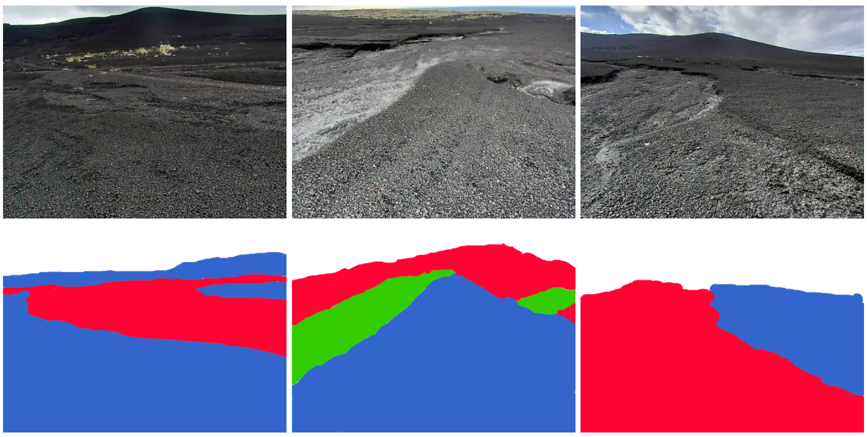

Fig. 5 Experimental fields with various soil types. Terrain types are labeled manually. (Green: Dense Sand, Blue: Fine Gravel, Red: Coarse Gravel)

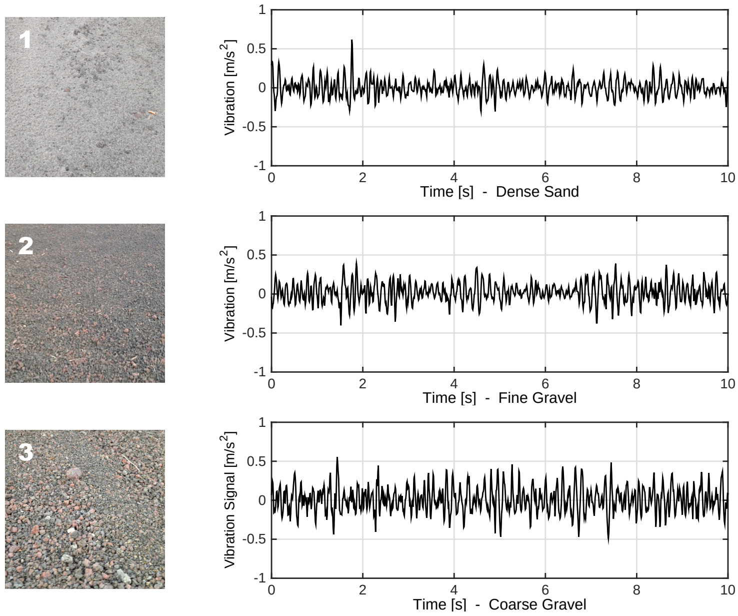

Fig. 6 Vibration signal example for 10 [s] traversal. Three terrain types are (1) Dense Sand, (2) Fine Gravel, and (3) Coarse Gravel. Each terrain presents distinct properties in signal strength, periodicity, etc.

eter Crossbow CXL17LF3 measures vibration data at 100 [Hz]. The consumption energy is computed from motor currents.

Izu-Oshima island in Japan is selected as the experimental field. The formation of the place is based on an active volcano Mt. Mihara. The geological features have been created by volcanic eruptions and water penetrations; therefore, diverse soil types are mixed in local regions. Three terrain types that can be seen in Fig. 5 are defined as follows.

1. **Dense Sand**: very small particles are packed and form hard terrain.
2. **Fine Gravel**: gravels of a few centimeters are loosely packed.
3. **Coarse Gravel**: larger gravels are piled and form deformable terrain.

The detailed appearance and sample vibration data are shown in Fig. 6. Each terrain types have distinct signal properties in terms of strength, periodicity, and so on.

The algorithm is implemented in MATLAB. For the wavelet transform to extract features, the software provided in [18] is used. The Morlet wavelet is selected as the mother wavelet. For the terrain classification, LIBSVM [6] is used. It employes the radial basis function kernel with optimal parameters tuned by 5-fold cross validation.

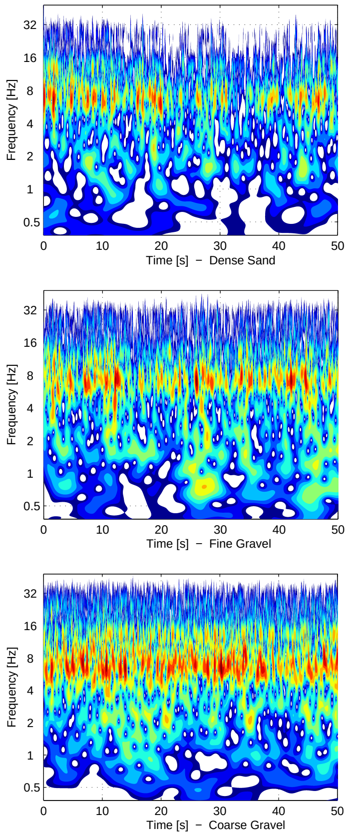

Fig. 7 Wavelet analysis of vibration signals for 50[s]. The signal power corresponding to the natural frequency $f_n = 6.8$ [Hz] and its octave $2f_n$ shows significant characteristics.

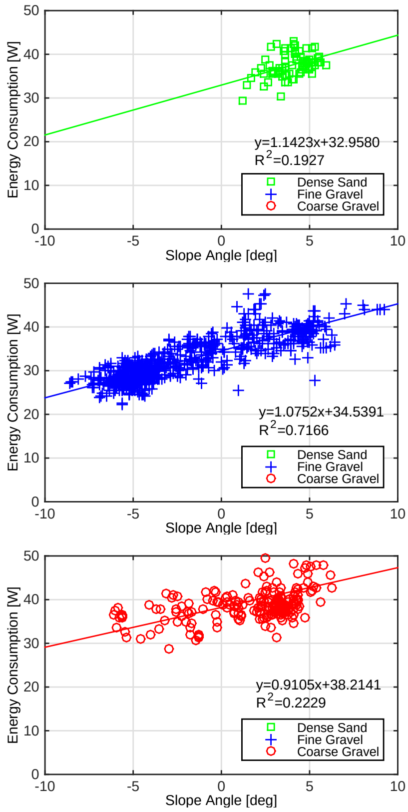

Fig. 8 Relationship between slope angle and energy consumption for 1 [m] traversal on natural terrain. The linearity can be observed in every terrain types. The estimated constants are shown in the figure.

4.2 Classifying Terrain based on Vibration Signals

The wavelet transform results for various terrain (i.e., $\boldsymbol{A}$) are shown in Fig. 7. The natural frequency $f_n = 6.8$ [Hz] and its octave show significant properties. Time-domain periodicity can be observed in correspondence with the grouser-to-grouser interval $t_g = 0.63$ [s]. In the algorithm, 2×20 matrices are extracted from these results to generate 8-element feature vectors.

The classification result by the vibration-based classifier is shown in Table 1. The dataset size is 191, 300, and 225, respectively. In the experiment, 10-fold cross validation is used to compute the average accuracy and variance. The 64-point FFT features similar to [15, 19] are used as reference. The accuracy was 76.80% for 3-class classification which is slightly inferior to the FFT features. However, the difference

Table 1 Classification rates per class and total classification accuracy (%) in 10-fold cross validation.

	Proposed	64pt-FFT
Dense Sand	97.21 ± 1.85	95.45 ± 3.71
Fine gravel	79.59 ± 5.42	86.81 ± 8.42
Coarse gravel	83.80 ± 3.38	80.90 ± 7.67
Total	76.80 ± 4.59	78.18 ± 7.67

Table 2 Confusion matrix for test data.

	Dense Sand	Fine gravel	Coarse gravel	Unclassified
Sand	**93.71**	2.63	0.53	3.13
Fine gravel	1.67	**81.00**	8.33	9.00
Coarse gravel	2.23	30.61	**58.74**	8.42

is small considering the number of elements is eight times smaller. Moreover, higher classification accuracy is achieved for some classes. In fact, the error rate for dense sand terrain is less than 3%.

The confusion matrix for 3-class test data is shown in Table 2. There is confusion in fine and coarse gravels. This is because the separability in the feature space was relatively small. One reason will be the ambiguity of human hand-labeling. Introducing pre-training and new data might improve the classification.

4.3 Modeling Energy Usage

Two parameters $\alpha_{r,t}$ and $\delta_{r,t}$ in the energy consumption model in (11) is empirically estimated. From average consumption of all 1 [m] segments in a 773 [m] trajectory, the linear regression model is estimated. Obtained data points and parameters are presented in Fig. 8. The result shows that the terrain in the largest consumption (coarse gravel) requires more than 15% times grater than the smallest (dense sand). This fact supports the importance of distinguishing classes in the energy-aware context.

Along with the vibration-based classifier, these regression functions produce the energy estimation using a vibration sensor and slope measurement. Fig. 9, 10, and 11 present the results for three 100 [m] paths. Although terrain has various elevation profiles, the energy estimates were accurate. The RMS errors are 3.42, 3.06, 5.56 [W] for three paths. The reason for worse performance in Fig. 11 is that geometrical steps caused wheel stuck at around 700 and 1000 [s], resulting in the rapid increase of energy consumption. In addition to the soil type classification, the importance of geometrical hazard estimation is suggested.

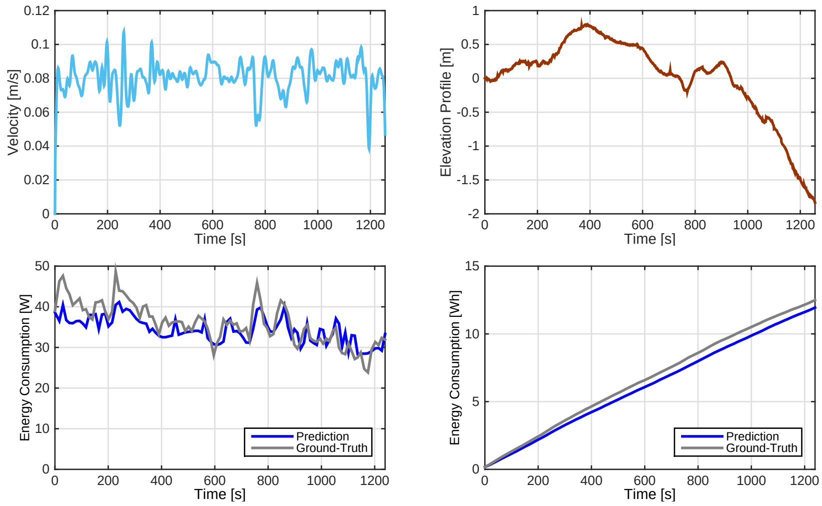

Fig. 9 Experimental result for path 1. Top row: actual velocity (left) and elevation profile (right). Bottom row: Comparison between predicted and measured energy consumption (left) and its integral (right).

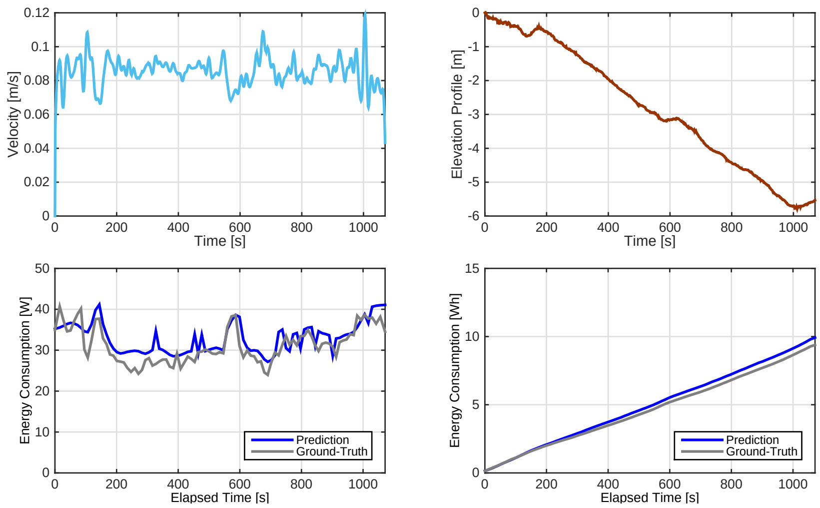

Fig. 10 Experimental result for path 2.

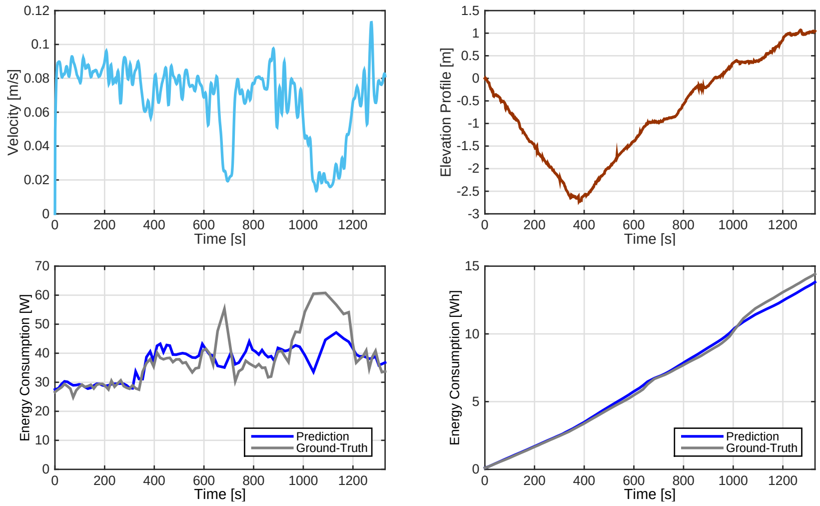

Fig. 11 Experimental result for path 3. Note that the error grows at 700 and 1000 [s] due to the geometrical step hazards.

5 Conclusion

This paper presented an approach to estimate the energy consumption of mobility systems using vibration-based terrain classification. The compact feature representation in the time-frequency domain shows accurate classification performance in the multi-class labeling problem. The classification results are combined with the regression model considering a simple physical model to estimate actual energy consumption. The real field data validate the promising performance of the proposed vibration-based approach.

Several improvements can be suggested to the current inference model. As the experiments showed, the energy consumption drastically changes in the presence of (non-)geometrical hazards such as steps or slip-inducing terrain. The regression model should consider those hazards in order to improve robustness. Moreover, the confusion in similar terrain types may be improved by introducing pre-training, or handling visual information at the same time.

References

1. Angelova, A., Matthies, L., Helmick, D., Perona, P.: Learning and prediction of slip from visual information. Journal of Field Robotics **24**(3), 205–231 (2007)
2. Biesiadecki, J., Maimone, M.: The Mars Exploration Rover surface mobility flight software: driving ambition. In: IEEE Aerospace Conference (2006)
3. Brooks, C., Iagnemma, K.: Vibration-based terrain classification for planetary exploration rovers. IEEE Transactions on Robotics **21**(6), 1185–1191 (2005)

4. Brooks, C., Iagnemma, K., Dubowsky, S.: Vibration-based terrain analysis for mobile robots. In: IEEE International Conference on Robotics and Automation, pp. 3415–3420 (2005)
5. Brooks, C.A., Iagnemma, K.: Self-supervised terrain classification for planetary surface exploration rovers. Journal of Field Robotics **29**(3), 445–468 (2012)
6. Chang, C., Lin, C.: LIBSVM: a library for support vector machines (2001). URL http://www.csie.ntu.edu.tw/ cjlin/libsvm
7. Coyle, E., Collins, E.: A comparison of classifier performance for vibration-based terrain classification. In: 26th Army Science Conference (2008)
8. DuPont, E.M., Moore, C.A., Collins, E.G., Coyle, E.: Frequency response method for terrain classification in autonomous ground vehicles. Autonomous Robots **24**(4), 337–347 (2008)
9. Iagnemma, K.D., Dubowsky, S.: Terrain estimation for high-speed rough-terrain autonomous vehicle navigation. In: SPIE Conference on Unmanned Ground Vehicle Technology IV, vol. 4715, pp. 256–266 (2002)
10. Krebs, A., Pradalier, C., Siegwart, R.: Adaptive rover behavior based on online empirical evaluation: Rover-terrain interaction and near-to-far learning. Journal of Field Robotics **27**(2), 158–180 (2010)
11. Maimone, M., Biesiadecki, J.J., Tunstel, E., Cheng, Y., Leger, C.: Surface navigation and mobility intelligence on the Mars Exploration Rovers. In: A. Howard, E. Tunstel (eds.) Intelligence for Space Robotics, chap. 3, pp. 45–69 (2006)
12. Ojeda, L., Borenstein, J., Witus, G., Karlsen, R.: Terrain characterization and classification with a mobile robot. Journal of Field Robotics **23**(2), 103–122 (2006)
13. Otsu, K., Otsuki, M., Kubota, T.: A comparative study on ground surface reconstruction for rough terrain exploration. In: International Symposium on Artificial Intelligence for Robotics and Automation in Space (2014)
14. Rakhmatov, D., Vrudhula, S.: Energy management for battery-powered embedded systems. ACM Transactions on Embedded Computing Systems **2**(3), 277–324 (2003)
15. Sadhukhan, D.: Autonomous Ground Vehicle Terrain Classification Using Internal Sensors. Master's thesis, Florida State University (2004)
16. Sadhukhan, D., Moore, C., Collins, E.: Terrain estimation using internal sensors. In: IASTED International Conference on Robotics and Applications (2004)
17. Stavens, D., Thrun, S.: A self-supervised terrain roughness estimator for off-road autonomous driving. In: Annual Conference on Uncertainty in Artificial Intelligence (2006)
18. Torrence, C., Compo, G.P.: A Practical Guide to Wavelet Analysis. Bulletin of the American Meteorological Society **79**(1), 61–78 (1998)
19. Weiss, C., Fechner, N., Stark, M., Zell, A.: Comparison of Different Approaches to Vibration-based Terrain Classification. In: European Conference on Mobile Robots, pp. 7–12 (2007)
20. Weiss, C., Frohlich, H., Zell, A.: Vibration-based terrain classification using support vector machines. In: IEEE/RSJ International Conference on Intelligent Robots and Systems, pp. 4429–4434 (2006)